Wide-pressure-range coplanar dielectric barrier discharge: Operational characterisation of a versatile plasma source

J. Čech, Z. Bonaventura, P. Sťahel, M. Zemánek, H. Dvořáková, and M. Černák

Citation: Phys. Plasmas **24**, 013504 (2017); doi: 10.1063/1.4973442
View online: http://dx.doi.org/10.1063/1.4973442
View Table of Contents: http://aip.scitation.org/toc/php/24/1
Published by the American Institute of Physics

Wide-pressure-range coplanar dielectric barrier discharge: Operational characterisation of a versatile plasma source

J. Čech,[a] Z. Bonaventura, P. Sťahel, M. Zemánek, H. Dvořáková, and M. Černák
CEPLANT–R&D Centre for Low-Cost Plasma and Nanotechnology Surface Modifications, Masaryk University, Kotlářská 2, 611 37 Brno, Czech Republic

(Received 26 September 2016; accepted 15 December 2016; published online 6 January 2017)

Many plasma applications could benefit from the versatile plasma source operable at a wide-pressure-range, e.g., from the fraction of Pa to the super-atmospheric conditions. In this paper, the basic characteristics of wide-pressure-range plasma source based on the coplanar dielectric barrier discharge is given. The operational characteristics of this plasma source were measured in nitrogen at pressures ranging from 10^{1} Pa (resp. 10^{-4} Pa) to 10^{5} Pa. Measurements of the plasma geometry, breakdown voltage, and micro-discharges' behaviour revealed three operational regimes of this plasma source: "high pressure," "transitional" and "low-pressure" with vague boundaries at the pressures of approx. 10 kPa and 1 kPa. It was found that the plasma layer of coplanar dielectric barrier discharge could be expanded up to several centimetres to the half-space above the planar dielectric barrier when the gas pressure is reduced below 1 kPa, which provides an outstanding space to tailor the source for the specific applications. The proposed model of an effective gap distance in the Paschen breakdown criterion enabled us to explain the discharge behaviour fitting the experimental breakdown voltage data in the whole studied pressure range. Under the filament-forming conditions, i.e., at the pressure range from approx. 1–100 kPa, the active plasma volume could be varied through the micro-discharges' lateral thickness scaling with the inverse of the square-root of the gas pressure. *Published by AIP Publishing.*
[http://dx.doi.org/10.1063/1.4973442]

Up till now, the dielectric barrier discharges[1] (DBDs) were studied preferably at atmospheric pressure conditions attractive to industrial users in that they avoid the high engineering costs usually associated with vacuum-based plasmas.[2–5] At other than under very specific operating conditions and limited gas compositions,[6] atmospheric pressure DBDs consist of arrays of filamentary or "microstreamer" discharges. However, for most particularly surface treatment applications, uniform, non-filamentary discharges are more effective[7] and consequently the goal is to avoid plasma filamentation. To optimize the plasma treatment particularly of porous materials, the scientific interest was turned also to the properties of DBDs at lower (sub-atmospheric) gas pressures.[8] However, there exists a broader potential for the DBD when operated as the versatile wide-pressure-range (WPR) plasma source.

Two spatial configurations of DBD have been studied at sub-atmospheric pressure so far. The first and the most common configuration is volume DBD, which was used for: (i) basic plasma diagnostics at selected low-pressure values;[9–12] (ii) plasma assisted chemical vapour depositions at low-pressures;[13] (iii) novel ionization source for mass spectrometry;[14] and (iv) textile treatment.[8] The second DBD configuration tested at sub-atmospheric pressure was surface DBD used for plasma actuators.[15,16]

To our best knowledge, the DBD in coplanar configuration has not been studied at low-pressure conditions so far (except for plasma display panels[17,18]), despite its indisputable potential for plasma diagnostics (see, e.g., our recent work on the residual heat contribution to the "memory effect"[19] or surface charges recombination dynamics[20]) and also for the potential in applications, e.g., for plasma cleaning[21] or thin film deposition, like atomic layer deposition (ALD).[22–24] Coplanar dielectric barrier discharge (CDBD) possesses two main beneficial features for these practical applications: (i) contrary to the volume DBD, an open geometry of CDBD electric field enables the undisturbed view on the whole process of plasma formation and the discharge evolution along the solid dielectrics (see, e.g., Ref. 20) and from the application point of view, this open geometry puts no constrains on the thickness of treated material; (ii) unlike surface DBD, CDBD has no bare metal electrodes exposed to the plasma. Thus the lifetime of CDBD is not limited by electrode sputtering, and the absence of sputtering allows its use for scenarios, where the sputtered material could introduce undesired contamination, either in plasma diagnostics, or in applications.

The construction of common CDBD plasma sources (e.g., plasma display panels[17,18] or ozone generators[25]) involves thin insulation dielectric layer and narrow electrode gaps in the order of 10–100 μm. While such design reduces the breakdown voltage, it concurrently reduces the amount of transferred charge, which limits substantially the magnitude of total released energy. Lowering the pressure would inevitably lead to even more pronounced reduction of deposited power.

A more suitable geometry for the adoption at the wide-pressure-range (WPR) DBD plasma source is that of the

[a]Electronic mail: cech@physics.muni.cz

so-called Diffuse Coplanar Surface Barrier Discharge (DCSBD).[26] The DCSBD utilizes the extended electrode gaps of the order of 0.1–1 mm, which increases considerably the amount of charge transferred and so the energy released. Wider electrode gaps also enable operation of the plasma source on the descending (right) branch of the Paschen curve across the wider pressure range. Although this poses higher demands on the quality of electrical insulation, it was solved on the laboratory scale at the moment, giving room for testing emerging applications. Resulting WPR-CDBD consisted of three electrode pairs embedded in glass–ceramic dielectrics. The electrodes of 45 mm length and 1.5 mm thickness were formed into an "inter-digital transducer (IDT)" pattern with inter-electrode distance of 1 mm. The electrode length and the number of electrode pairs were chosen to form a compact, yet full-featured, plasma source suitable for plasma diagnostics.

To study its performance and characteristics at reduced pressures, the WPR-CDBD was mounted in the vacuum chamber made of a glass cylinder with quartz glass window mounted on top of the chamber ("top-view"). Vacuum bushings for high-voltage (HV) cables and water cooling system were mounted onto the bottom of the chamber. Vacuum conditions were maintained using Scroll pump. The chamber pressure was measured using resistive (Pirani) and capacitive (Baratron) gauges. Working gas pressure was controlled using a needle valve. The system was evacuated to approx. 10 Pa and flushed with nitrogen (purity 99.999%) several times prior the measurements. For tests down to 10^{-4} Pa, the stainless steel vacuum chamber with two-stage turbomolecular/Scroll pumps was used, but this system did not allow to settle the fixed gas pressure in the chamber, and the presence of the grounded chamber surface changes the discharge conditions considerably. Therefore the results for pressures below 30 Pa are not presented here.

The schematic of the whole experimental setup is shown in Figure 1. The custom-made tunable high-voltage (HV) generator was used. The generator output HV of sine waveform. In the present study, a frequency of 40 kHz was used. The arbitrary function generator Agilent 33220A was used as the reference clock signal for HV generator and, simultaneously, as the triggering signal for intensified CCD (ICCD) camera. This enabled us to take the phase-locked images of the discharge pattern with respect to the current waveform of the discharge.

The phase-locked imaging was performed using ICCD camera sensitive in the range from 200 to 900 nm and equipped with macro lens (Princeton Instruments PI-MAX3 1024i-SR-46; SIGMA 105 mm 1:2.8 DG MACRO EX). Discharge patterns of single or half-period of the discharge were captured. Dimensions of the plasma layer were investigated using cross-imaging of the discharge pattern in top and side view using synchronized DSLR cameras (Nikon N80/ SIGMA 105 mm 1:2.8 DG MACRO EX and N5100/ NIKKOR 50 mm f/1.8D AF). Micrometric positioning plate (Manfrotto 454) was used to focus on the plasma layer from the top-view.

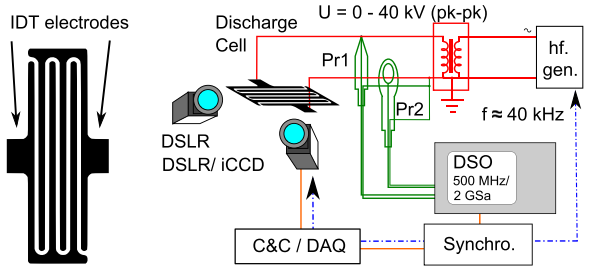

FIG. 1. Top-view of IDT electrodes geometry of WPR-CDBD (left); whole experimental set-up (right).

The WPR-CDBD plasma source was studied in the working gas pressure from 30 Pa up to 0.13 MPa, but the operability was tested down to 10^{-4} Pa, i.e., in nearly 9 orders of magnitude of working gas pressure. The breakdown voltage, plasma dimensions, and micro-discharges' (MDs) behaviour were investigated as a function of the gas pressure.

Three "pressure" regimes of the WPR-CDBD were identified, according to the discharge parameters and behaviour: (a) the "high-pressure"; (b) "transitional" and (c) "low-pressure" regimes. The appearance of discharge in these regimes is shown in Figure 2. "High-pressure" regime represents the appearance of WPR-CDBD at atmospheric and super-atmospheric pressures. At "high-pressure" regime, the discharge consisted of numerous thin micro-discharges (MDs) branched above electrodes and burning at the nanosecond time scale forming a sub-millimetre thin plasma layer. This is a typical operation regime for standard DBD.[27]

When the pressure was decreased bellow approx. 10–20 kPa, the "transitional" regime occurred. Even though the individual MDs were still present in the discharge volume, their appearance changed considerably. They formed wide diffuse structures above electrodes with no branching. However, the plasma layer thickness did not change considerably, being still at the sub-millimetre range.

When the gas pressure was reduced below approx. 1 kPa, the character of WPR-CDBD had changed completely and the discharge entered its "low-pressure" regime of operation. At the "low-pressure" regime, the discharge expanded

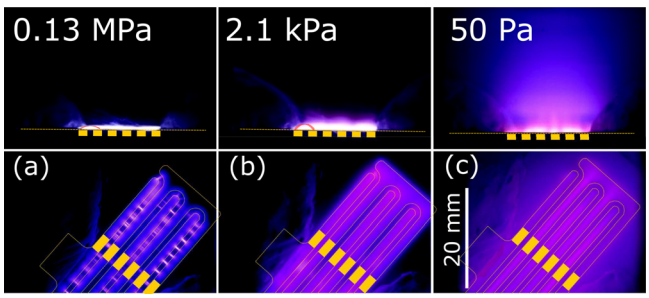

FIG. 2. Images of plasma in (a) "high-pressure"; (b) "transitional" and (c) "low-pressure" regime shown from two directions: The side-view (top images) represents the view on the discharge from the perspective parallel to the dielectric plate. The position of the dielectrics-gas boundary (orange dashed line) together with the position of the electrodes under the dielectric surface (orange rectangles) are given. The vertical plasma shape ("arching") is highlighted using red color. The top-view (bottom images) represents the view on the discharge from the perspective perpendicular to the dielectric plate. The position of the electrodes under the surface of the dielectrics are given in contours (orange dash lines). The scale bar representing 20 mm distance is given for comparison. (Contrast was enhanced for better visibility of plasma structures.)

to the half-space above the dielectric barrier. The sharply defined individual MDs were substituted by enlarging "glow" areas on the surface of dielectric barrier above the energizing electrodes. In the gas volume, the clearly visible plasma "plume" had developed at pressures around 50–100 Pa and vanished again at pressures below 50 Pa.

The working gas pressure is closely connected with the breakdown voltage and total energy released. In the classical theory of direct-current low-pressure discharge, this dependency is described by the Paschen law, which states the similarity law between the breakdown voltage U_b and the product of the pressure and the gap distance pd

$$U_b = \frac{Bpd}{\ln(Apd) - \ln(\ln(1 + 1/\gamma_{se}))}, \tag{1}$$

where A, B, and γ_{se} and are constants depending on gas composition and surface properties of electrodes or dielectric barriers.

Derivation of the Paschen law assumed a parallel plate geometry of discharge electrodes, which differs from our WPR-CDBD system. Therefore some adaptation to our geometry was necessary. Simple 2D electrostatic calculations showed that when the external voltage is applied to the WPR-CDBD electrode system, the electric field lines are "arched" in the gas above the dielectric plate (i.e., above the gaps formed by electrode pairs).[28] Thus the inter-electrode part of WPR-CDBD discharge is not formed directly at the surface of the dielectrics, but it is pushed to the half-space above the dielectric surface making it visually "arched" (see Figure 2). With decreasing pressure, the plasma layer "arching" becomes more pronounced. Finally in the "low-pressure" regime of operation, the plasma boundary becomes blurred and the plasma "plume" with diffusive boundary appears (compare the regimes in Figure 2). Experimentally observed vertical thickness of the plasma layer with respect to the working gas pressure is shown in Figure 3. Data of vertical thickness were estimated using 2% of the most luminous pixels from the side-view discharge photographs (see Figure 2). The vertical thickness of the plasma layer at pressure p could be approximated by empirical formula

$$f(p) = a/p + b, \tag{2}$$

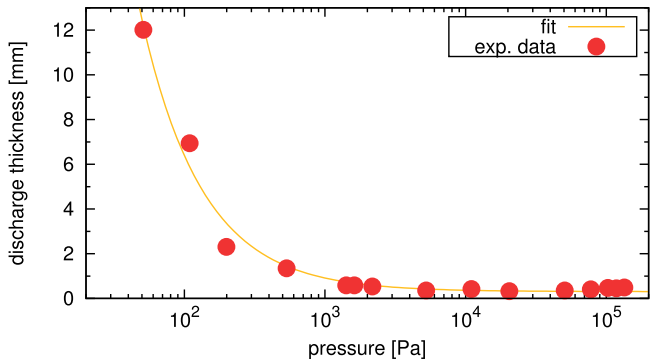

FIG. 3. Vertical thickness of the plasma layer as a function of pressure. Points represent the experimental data and the line is a formula $f(p) = a/p + b$ fitted with parameters $a = 0.61$ mPa and $b = 3.0 \times 10^{-4}$ m.

with $a = 0.61$ mPa and $b = 3.0 \times 10^{-4}$ m.

This allowed us to define an effective gap distance d_{eff} being proportional to the length of the arched plasma layer. The effective gap distance d_{eff} was then used instead of d in the Paschen law (1). The length of the plasma layer can be approximated by arc length of parabola with maximum at the vertical thickness of plasma layer $f(p)$ and intersecting electrode edges separated by distance 2ξ as

$$d_{eff}(p) \propto \sqrt{\xi^2 + 4f^2(p)} + \frac{\xi^2}{4f(p)} \ln\left(\frac{\sqrt{\xi^2 + 4f^2(p)} + 2f(p)}{\sqrt{\xi^2 + 4f^2(p)} - 2f(p)}\right), \tag{3}$$

with $\xi = 0.5$ mm corresponding to the half distance between the electrode edges that are fully immersed in the dielectrics, $f(p)$ is given by (2).

Figure 4 shows the measured experimental data for breakdown voltages as a function of the working gas pressure together with the model

$$U_b = \frac{\alpha p\, d_{eff}(p)}{\ln(\beta p\, d_{eff}(p))}, \tag{4}$$

with $\alpha = 421$ V Pa^{-1}m^{-1} and $\beta = 5.96$ Pa^{-1}m^{-1}. The standard Paschen's law form of (1) is shown as well for which the breakdown voltage diverges at pressures below 400 Pa.

The vertical thickness of the WPR-CDBD plasma layer (see Figure 3) is an important parameter for its intended applications. It can be seen that with the decrease of gas pressure, the thickness of plasma layer remained unchanged until the pressure of approx. 1 kPa had been reached. Then a steep increase of the thickness occurred. Experimental observations showed that the WPR-CDBD plasma layer started expanding to the half-space above the dielectric at the gas pressure below 200 Pa, losing its sharp vertical boundaries at pressure below 50 Pa (glow light in the whole chamber above the dielectrics).

The behaviour of individual MDs was investigated by ICCD imaging of single half-period at higher optical magnification. Their appearances at different gas pressures are shown in Figure 5. Sharp and branched discrete MDs were formed when the pressure is higher than 10–20 kPa; creating a thin, constricted channel as the streamer theory predicts.[29] When the gas pressure drops below approx. 10–20 kPa, the MDs' channels became wider and transformed from branched into the diffuse form, spreading along the electrodes. As the pressure decreased below approx. 1 kPa, the MDs became blurry and finally (if the input power was high enough) a continuous layer of plasma developed above the electrodes with pronounced high-intensity zones above the energizing electrodes resembling the cathode spots of low-pressure glow discharge.

Observed lateral structure of individual MDs (shown in Figure 5) allowed us to establish the dependence of MD diameter on gas pressure, see Figure 6. Two individual MDs produced during two consecutive half-periods of input HV were averaged (both reusing the same discharge path[30]). The diameter of MD was taken as the lateral thickness of the

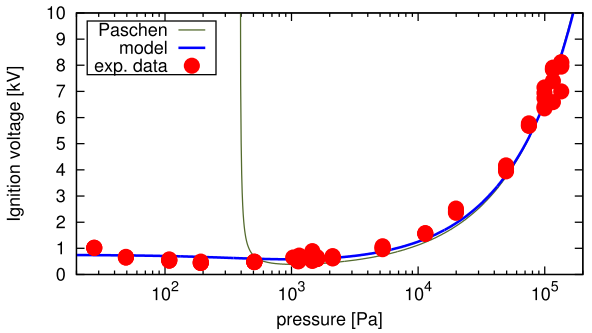

FIG. 4. Breakdown voltages as a function of the working gas pressure: experimental data (red points); breakdown voltages modelled by (4) (blue line); standard Paschen's law (1) (green line).

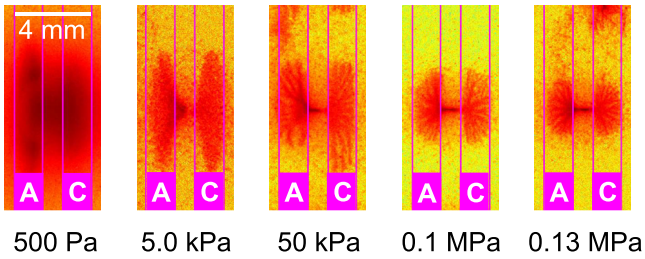

FIG. 5. ICCD images of individual MD with respect to the working gas pressure. Images taken in single half-period of the discharge. Polarity and edges of electrodes are labelled A (anode), C (cathode).

luminous channel (filament) at the half distance between electrode edges. The experimental data of MDs' diameter can be approximated by the power law formula

$$f(p) = a \times p^b, \tag{5}$$

with $a = 4.5 \times 10^{-2}$ m and $b = -0.50$. Based on the experimental data, we could conclude that the diameter of MD channel is inversely proportional to the *square-root* of pressure for the studied WPR-CDBD in the pressure range of 1–100 kPa. When we compared this result to the data in literature,[8,31–33] we have found that while the scaling factor for the diameter of streamers in free-space geometry (i.e., in volume DBD), is inversely proportional to the *first power* of pressure (or gas density) (see Refs. 31 and 32), there is a numerical model in Ref. 33 for the radius of discharge channel in volume DBD configuration based on the electron drift (diffusion) in radial direction that estimates the radius of MD channel to be inversely proportional to the *square-root* of pressure and directly proportional to the *square-root* of air

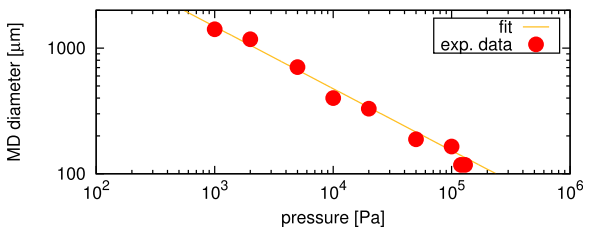

FIG. 6. Diameter of MDs as a function of pressure. Points represent the experimental data, and the line is a formula $f(p) = a \times p^b$ fitted with parameters $a = 4.5 \times 10^{-2}$ m and $b = -0.50$.

gap (electrode gap). The measured pressure dependence of MDs' diameter in WPR-CDBD agrees well with the formula in Ref. 33, proposed for volume DBD in air, taking into account the fact, that the measured WPR-CDBD discharge thickness in the pressure range of 1–100 kPa remains practically the same (see Figure 6) and thus we can assume the effective discharge gap to be close to the (fixed) electrode gap. Our results are qualitatively the same as those reported in Ref. 8 for volume DBD with the gas gap of 8 mm, although the measured data of the dependence of MD's diameter on the gas pressure are not given there to enable the direct comparison.

We can conclude, that a versatile wide-pressure-range plasma source based on coplanar dielectric barrier discharge (WPR-CDBD) was designed, and it proved its operability at the pressure range from mPa to MPa, without any design modification or ignition helpers, which is beneficiary not only from the point of view of plasma diagnostics and simulation, but also from the point of view of the prospective applications. The results of plasma diagnostics were given in the range from 10^1 Pa to 10^5 Pa, i.e., in the span of more than 4 orders of pressure magnitude. As the pressure decreases, the WPR-CDBD transits from filamentary regime with a thin layer of individual micro-discharges to the diffuse "glow-like" regime of thick plasma layer with luminous zones on the dielectric above electrodes (cathode spots). The thickness of plasma layer can be easily manipulated from some 100 μm up to several centimetres only by the change of the gas pressure. Finally the discharge can be triggered on timescale from milliseconds up, enabling a precise modulation of the plasma for diagnostics and also for the intended plasma treatment applications of presented WPR-CDBD plasma source, which are beyond the scope of the presented paper. To name at least one particular and very interesting application of the WPR-CDBD plasma source, we could mention the application of WPR-CDBD as the plasma decontaminator of vacuum chambers of the Scanning Electron Microscope, which has been already successfully investigated and where the pressure–distance operational conditions could be easily tailored for the best contamination removal effects (see Ref. 34).

This research has been supported by the Project No. CZ.1.05/2.1.00/03.0086 funded by the European Regional Development Fund and Project No. LO1411 (NPU I) funded by the Ministry of Education Youth and Sports of Czech Republic and by the Project No. GA13-24635S of the Czech Science Foundation.

[1]U. Kogelschatz, B. Eliasson, and W. Egli, J. Phys. IV France **7**, C4-47 (1997).
[2]U. Kogelschatz, Plasma Chem. Plasma Process. **23**, 1 (2003).
[3]H.-E. Wagner, R. Brandenburg, K. V. Kozlov, A. Sonnenfeld, P. Michel, and J. F. Behnke, Vacuum **71**, 417 (2003).
[4]P. Bruggeman and R. Brandenburg, J. Phys. D: Appl. Phys. **46**, 464001 (2013).
[5]M. Černák, D. Kováčik, J. Ráheľ, P. Sťahel, A. Zahoranová, J. Kubincová, A. Tóth, and Ľ. Černáková, Plasma Phys. Controlled Fusion **53**, 124031 (2011).
[6]F. Massines, N. Gherardi, N. Naudé, and P. Ségur, Eur. Phys. J. Appl. Phys. **47**, 22805 (2009).
[7]F. Massines and G. Gouda, J. Phys. D: Appl. Phys. **31**, 3411 (1998).

[8]N. De Geyter, R. Morent, and C. Leys, Plasma Sources Sci. Technol. **15**, 78 (2006).
[9]E. Wagenaars, R. Brandenburg, W. J. M. Brok, M. D. Bowden, and H.-E. Wagner, J. Phys. D: Appl. Phys. **39**, 700 (2006).
[10]R. Brandenburg, M. Bogaczyk, H. Höft, S. Nemschokmichal, R. Tschiersch, M. Kettlitz, L. Stollenwerk, T. Hoder, R. Wild, K.-D. Weltmann, J. Meichsner, and H.-E. Wagner, J. Phys. D: Appl. Phys. **46**, 464015 (2013).
[11]H. Höft, M. Kettlitz, K.-D. Weltmann, and R. Brandenburg, J. Phys. D: Appl. Phys. **47**, 455202 (2014).
[12]H. Khatun, A. K. Sharma, and P. K. Barhai, Braz. J. Phys. **40**, 450 (2010).
[13]D. Liu, T. Ma, S. Yu, Y. Xu, and X. Yang, J. Phys. D: Appl. Phys. **34**, 1651 (2001).
[14]M. Sugiyama, S. Kumano, K. Nishimura, H. Hasegawa, and Y. Hashimoto, Rapid Commun. Mass Spectrom. **27**, 1005 (2013).
[15]J. Soni and S. Roy, Appl. Phys. Lett. **102**, 112908 (2013).
[16]X. Che, W. Nie, T. Shao, X. Tian, Z. Hou, H. He, P. Zhou, S. Zhou, and Ch. Yang, Phys. Plasmas **21**, 043508 (2014).
[17]J. P. Boeuf, J. Phys. D: Appl. Phys. **36**, R53 (2003).
[18]J.-W. Ok, B.-S. Lee, S. Choi, M.-S. Won, D.-H. Kim, H.-J. Lee, and H.-J. Lee, Plasma Sources Sci. Technol. **23**, 025018 (2014).
[19]J. Ráheĺ, Zs. Szalay, J. Čech, and T. Morávek, Eur. Phys. J. D **70**, 92 (2016).
[20]T. Morávek, J. Čech, Z. Navrátil, and J. Ráheĺ, Eur. Phys. J. Appl. Phys. **75**, 24706 (2016).
[21]P. Krüger, R. Knes, and J. Friedrich, Surf. Coat. Technol. **112**, 240 (1999).
[22]S. M. George, Chem. Rev. **110**, 111 (2010).
[23]E. S. Brandt and J. M. Grace, J. Vac. Sci. Technol., A **30**, 01A137 (2012).
[24]D. Theirich, R. Müller, K. Zilberberg, S. Trost, A. Behrendt, and T. Riedl, Chem. Vap. Deposition **19**, 167 (2013).
[25]V. I. Gibalov, T. Murata, and G. J. Pietsch, Ozone Sci. Eng. **25**, 431 (2003).
[26]M. Šimor, J. Ráheĺ, P. Vojtek, M. Černák, and A. Brablec, Appl. Phys. Lett. **81**, 2716 (2002).
[27]T. Hoder, R. Brandenburg, R. Basner, K.-D. Weltmann, K. V. Kozlov, and H.-E. Wagner, J. Phys. D: Appl. Phys. **43**, 124009 (2010).
[28]J. Čech, M. Zemánek, P. Stáhel, H. Dvořáková, and M. Černák, Acta Polytech. **54**, 383 (2014).
[29]Yu. P. Raizer and E. M. Bazelyan, *Lightning Physics and Lightning Protection* (Institute of Physics Publishing, Bristol, UK, 2000).
[30]J. Čech, J. Hanusová, P. Stáhel, and M. Černák, Open Chem. **13**, 528 (2014).
[31]P. Tardiveau, E. Marode, A. Agneray, and M. Cheaib, J. Phys. D: Appl. Phys. **34**, 1690 (2001).
[32]V. P. Pasko, U. S. Inan, and T. F. Bell, Geophys. Res. Lett. **25**, 2123, doi:10.1029/98GL01242 (1998).
[33]D. Braun, U. Küchler, and G. Pietsch, J. Phys. D: Appl. Phys. **24**, 564 (1991).
[34]J. Dugáček, P. Stáhel, J. Čech, and J. Jurmanová, in *HAKONE XV: International Symposium on High Pressure Low Temperature Plasma Chemistry, Book of Contributed Papers*, Brno, Czech Republic, edited by M. Černák and T. Hoder, 11–16 September (2016), p. 287.